

Group and successive pair collisions in scattering of Cs⁺ ions by tungsten single crystals

V. I. Veksler and V. V. Evstifeev

Tashkent State University

(Submitted August 4, 1972)

Zh. Eksp. Teor. Fiz. 64, 568-575 (February 1973)

The fine structure of the energy spectra of Cs⁺ ions scattered by the {110}, {001} and {112} faces of a tungsten single crystal is investigated under conditions of sufficiently high angular and energy resolution. Angular dependences of the energy corresponding to various peaks in the scattered ion spectrum and on an angle of incidence of the primary ions on the target surface at a given scattering angle are derived. As a rule, the plots are bell-shaped. The model of group interaction between an ion and four or three lattice atoms and the model of pair double or triple collisions are used to explain the shifts of the bell-shaped curve peaks along the incidence-angle scale for various scattering atomic directions. Serious difficulties are encountered in an attempt to explain the data solely on the basis of the multiple collisions mechanism.

It is known^[1-4] that heavy ions having a large effective diameter and having initial energies $U \leq 1$ kV can be scattered as a result of strong simultaneous interaction with a group of lattice atoms ("group interaction"). One of us^[1] has shown that in the case of a particular arrangement of the crystal lattice relative to the momentum of the ion scattered by it, assuming a hard-sphere interaction, that the energy spectrum of the ions scattered in a given direction as a result of the group interaction should have a line structure. This result was later generalized to include the case of arbitrary arrangement of the initial momentum of the ion relative to the lattice^[2], and this premise was later on demonstrated also for the case of an arbitrary interaction potential^[3,4].

It was established at the same time^[5] that the energy spectrum should have a line structure also when the ion is scattered in a given direction as a result of successive collisions with individual atoms of the lattice ("multiple interaction").

Thus, the presence of a line structure in the spectrum and of other scattering characteristics at $U < 1$ kV is not an attribute of the mechanism of interaction of the ion with the lattice atoms, and there is not enough justification for discussing the causes of the formation of the line structure within the framework of only one of the indicated mechanisms (as is done, in particular, by Arifov and Aliev^[6] for $U = 25-5000$ eV and for multiple interaction).

By way of a criterion that makes it possible to separate ions scattered as a result of the action of both indicated mechanisms, we can use the dependence of the position W of the line in the energy spectrum on the angle χ of incidence of the primary ions on the surface of a single crystal as a fixed value of the scattering angle ψ . Although this dependence has a bell-shaped form^[3] which is approximately the same for the group as well as for the multiple scattering mechanism^[7], the position of its maximum and the tendency of this maximum to shift when the distance between the scattered atoms is changed turn out to be different in the two cases, making it possible to establish reliably the interaction mechanism.

Thus, for multiple pair collisions the position $\varphi = \varphi_0$ (φ is the "incidence angle" between the direction of the motion of the primary ion and the normal to the line join-

ing the centers of the scattering atoms), of the maximum of the bell-shaped curve $W(\varphi)$ should shift toward larger angles of incidence on going from the more densely packed chain of scattered ions to the less densely packed one. The largest incidence angle $\varphi_{0\infty}$ corresponds to scattering of the ion by atoms when these particles have infinitesimally small dimensions:

$$\varphi_{0\infty} = (\pi - \psi) / 2. \quad (1)$$

As to the group interaction, assuming elastic collisions of absolutely hard spheres, φ_0 can be determined from the formula of^[2]

$$\operatorname{tg} \varphi_0 = \frac{(W_0/U)^{1/2} \sin \psi}{1 - (W_0/U)^{1/2} \cos \psi}, \quad (2)$$

where U and W_0 are the energies of the ion before and after the scattering.

Our task was to study experimentally the energy of Cs⁺ ions scattered in a specified direction at different values of the incidence angle χ on the face of a single crystal, for the purpose of identifying the interaction mechanism for one or another peak in the spectrum. To increase the incidence-angle interval as much as possible, and also to eliminate effects connected in a number of cases with the influence of the surface on the motion of the scattered ion, the scattering surfaces were chosen to be the faces {110}, {001}, and {112} of single-crystal tungsten with a rotation axis $\langle 110 \rangle$.

1. INSTRUMENT AND EXPERIMENTAL TECHNIQUE

The instrument (Fig. 1) consisted of an ion source, an ion gun shaping a beam of primary ions incident on the investigated target, an analyzer of the scattered ions, and a system for their registration.

Cs⁺ ions were produced in a source S^[8] (based on the principle of surface ionization produced in dissociation of alkali-metal halides) and were accelerated in a planar field U that determined the energy of the primary ions; the field was applied between the source and an electrode D located 2.5 mm away. The ions passed through a hole in the electrode D (1.4 mm diam) and were focused with a spherical capacitor C₁^[9] on the investigated target T. The spread of the incidence angles of the ion beam on the flat surface of the target did not exceed $\Delta\chi = \pm 1.8^\circ$. A parallel-plate capacitor C₂ was used to adjust the primary-ion beam positron

relative to the analyzer by shifting the beam along the target. Holes G_1 , G_2 , G_3 , and G_4 , with respective diameters 5.0, 5.5, 6.0, and 7.0 mm, were cut in the auxiliary electrodes K, L, and M; the latter were of spherical segments with radii 15 and 18 mm and shielded in particular, the target from the external fields. The first two openings were covered with a nickel grid of 0.25 mm mesh and transmission 0.8, while the last two were covered with a tungsten grid of 0.8 mm mesh and transmission 0.95.

Under the experimental conditions, at $U = 400$ eV the ion current to the electrode D was $(1-1.5) \times 10^{-4}$ A, and the current density on the target was $j = 1.5 \times 10^{-5}$ A/cm² (the diameter of the ion beam at the target was 1.9 mm).

The target was a rectangular strip cut from a tungsten single crystal obtained by zone melting. Its surface was first finished mechanically and then polished in a 10% aqueous solution of NaOH. The final dimensions were $18 \times 2.5 \times 0.15$ mm. By rotating the target about its long axis (the $\langle 11\bar{0} \rangle$ direction, perpendicular to the plane of the figure) it was possible to vary the angle of incidence of the primary ions on the target surface ($-2^\circ \leq \chi \leq 78^\circ$, the angle χ is taken to be positive if the primary and analyzed secondary ions move in opposite directions of the normal to the surface). The error in the determination of the zero of the angle χ was $\pm 1.5^\circ$. The faces $\{100\}$, $\{001\}$, and $\{112\}$ of the single crystal coincided with the surface of the target in such a way that the angle φ of incidence of the primary ions on the faces was equal to χ . The primary and investigated scattered ions moved in the $\{11\bar{0}\}$ plane. The target could be heated to incandescence by passing current through it, and under the experimental conditions ($T = 2000^\circ$ K) the voltage drop across its working part, the center of which had the potential of the electrode L, did not exceed 0.1 V.

A fraction of the scattered Cs^+ ions passed through windows G_3 and G_4 into an electrostatic analyzer with axis inclined at a fixed angle to the average direction of the primary-ion momentum (scattering $\psi = 92^\circ$). After passing through a drift space 254 mm long (cylinders $E_1 - E_3$ with diaphragms with apertures of 4.5 mm diameter, serving to exclude particles scattered by the walls), the analyzed ions were incident on the entrance diaphragm D_1 of the analyzer, with an aperture of variable diameter b' ; this diameter, together with the dimension of the working part of the target, determined the spread of the ion scattering angles ($b' = 0.9$ mm and $\Delta\psi = \pm 0.3^\circ$ under the operating conditions). The ions then entered the field of the spherical capacitor-analyzer C_3 , with a deflection angle 70° , an average radius of curvature

120 mm, and a distance 8 ± 0.05 mm between electrodes. The calculated energy resolution of the analyzer was $130^{[9]}$, and the value obtained by calibrating the instrument with thermal ions was ~ 125 at ion energies $U \geq 80$ eV, but decreased at $U < 80$ eV. The use of spherical capacitors C_1 and C_3 greatly increased the transmission of the setup. After being deflected in capacitor C_3 , the ions passed through the space bounded by the screening electrodes E_5 and E_6 and were directed by parallel-plate capacitor C_4 into the aperture of the exit diaphragm D_2 with variable diameter b'' ($b'' = 1$ mm under the operating conditions).

To increase the transmission of the setup, it was possible to apply potential differences between the electrodes K, L, and M as well as between E_1 , E_2 , and E_3 . Under the experimental conditions, however, the line along which the ions moved in the instrument from the target through windows G_3 and G_4 to the diaphragm D_2 was at a constant potential.

After passing through diaphragm D_2 , the ions were accelerated to a VEU-OT-8M copper-beryllium electron multiplier operating in conjunction with a U1-2 electro-metric amplifier connected to an ÉPP-09 automatic potentiometer, which was modified to be able to plot the current-voltage characteristics. The minimum sensitivity of the recording system was $10^{-17} - 10^{-18}$ A/mm.

The instrument was evacuated with mercury-vapor pumps. Before operation, the left-hand side of the instrument, up to diaphragm D_1 , was outgassed for a long time in an oven at $T = 300^\circ$ C, the electrodes D, C_1 , and L were heated by electron bombardment, and the target was outgassed at $T = 2300^\circ$ C. Under the working conditions, the residual-gas pressure measured by the flash method^[10] from their adsorption by the target was 6×10^{-8} Torr with the ion source turned on.

Since the energy interval of the ions entering the recording device was proportional in the described system to the ion energy W , the current-voltage characteristics must be divided by W to obtain the form of the energy spectrum. The spectra shown in Fig. 2 were not corrected by the indicated method. This correction was introduced, however, in all cases when the positions of the maxima in the spectra were determined.

We recorded and processed altogether about 2000 energy spectra.

2. RESULTS AND DISCUSSION

To assess the character of the displacements of the peaks in the energy spectra following a change in the incidence angle χ , Fig. 2 shows a series of such spectra for different χ obtained by scattering Cs^+ ions from the $\{110\}$ face ($U = 580$ eV). It follows indeed from the presented data that the displacements of the different peaks differ in character (Fig. 3).

Under real conditions, the peaks in the spectra have finite widths, owing to the spread of the angles ψ and χ in the instrument, to the additional scattering of the ions at very small angles, thermal vibrations of the atoms in the lattice, etc.

The position of peak I (Fig. 3) on the energy scale, within the range of angles χ at which it does not overlap appreciably other peaks ($11 \ll \chi \ll 57^\circ$), remains practically constant. The same occurs when the ions are scattered by the faces $\{001\}$ ($U = 500$ eV, $16 \leq \chi \leq 48^\circ$ —

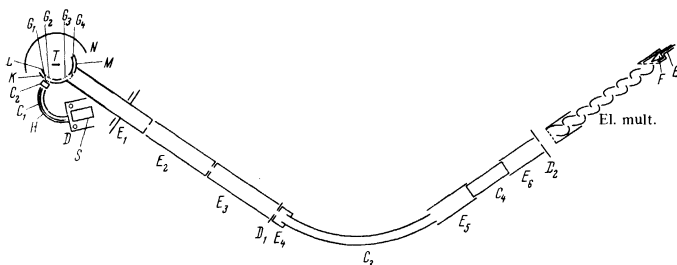


FIG. 1. Experimental setup: S—thermionic source; D—accelerating electrode; C_1 , C_3 —spherical capacitors; C_2 , C_4 —parallel-plate capacitors; K, L, M—guard electrodes; T—target, $E_1 - E_3$ —drift-space cylinders; D_1 and D_2 —entrance and exit diaphragms; H, N, E, $E_4 - E_6$ —screens; F—Faraday cylinder; G_{1-4} —windows.

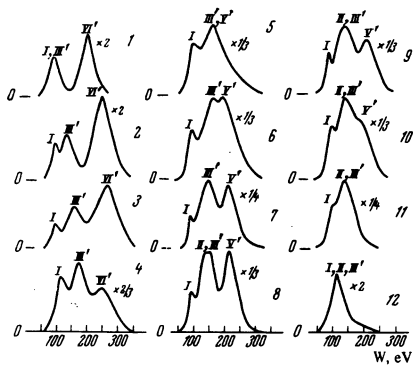


FIG. 2. Energy distributions (in arbitrary units) of Cs^+ ions scattered by the $\{110\}$ face of single-crystal tungsten, multiplied by W , at different angles χ (deg): 1) 11; 2) 15; 3) 19; 4) 25; 5) 29; 6) 33; 7) 37; 8) 41; 9) 47; 10) 51; 11) 59; 12) 71 ($U = 580$ eV).

Fig. 4) and $\{112\}$ ($U = 580$ eV, $10 \leq \chi \leq 24^\circ$ and $66 \leq \chi \leq 76^\circ$ —Fig. 5). The energies W_{0T} of the scattered ions, calculated from the elementary formulas for pair interaction at $U = 500$ eV ($W_{0T} = 78$ eV) and $U = 580$ eV ($W_{0T} = 87$ eV) are close to those obtained in experiment (80 and 90 eV, respectively). All this enables us to ascribe peak I to single paired scattering of the ion by an unbound lattice atom. Some increase in the energy W_0 at angles $\chi < 31^\circ$ (Fig. 3) may be due to the additional scattering action of the surface atoms on the ion in question, which moves under these conditions practically along the surface.

The bell-shaped curves IV and V (Fig. 4) can be attributed to double paired scattering of the ions by lattice atoms belonging to the close-packed directions $[111]$. However, by virtue of crystallographic-symmetry considerations, the distance between the indicated curves should be 71° , whereas experiment yields 55° . This fact cannot be attributed to the additional scattering action of other surface atoms, since the transition from the scattering surface of the face $\{001\}$ to the face $\{112\}$ is accompanied by shifts of 35° and 37° in the maxima of curves III and IV, respectively, in good agreement with the value 35° dictated by crystal-geometry considerations.

It might be assumed that the onset of peaks IV is due to paired interaction of the ion with atoms 1 and 2 of the $\langle 111 \rangle$ chain (Fig. 6). The angular displacement of the maximum of its bell-shaped curve relative to the normal to the $\langle 111 \rangle$ line joining the centers of the scattering atoms is then $\varphi_0 = \chi_0 - 35^\circ = 26^\circ$. But there is no analogous bell-shaped curve ($\chi_0 = \varphi_0 = 26^\circ$) connected with scattering by atoms 1 and 3 in the case of the third target (Fig. 5). In addition, in the case of the first target (Fig. 3), no bell-shaped curve ($\varphi_0 \sim 25-30^\circ$) is observed for the most probable scattering, which in this case is double scattering by atoms 4 and 5 belonging to the $\langle 00\bar{1} \rangle$ direction. Finally, an estimate of the pair-interaction potential on the basis of the experimental value of $\varphi_0^{[11]}$ gives a value that greatly overestimates the effective diameters of the interacting particles. It must therefore be assumed that it is the bell-shaped curve V which is connected with the double paired interaction (Figs. 4 and 5).

The maximum of this curve is separated from the normal to the $\{112\}$ plane in which the scattering directions $\langle 1\bar{1}1 \rangle$ lie by an angle $\bar{\varphi}_0 = 42^\circ$ ($\varphi_0 = 41^\circ$ for Fig. 4 and $\varphi_0 = 43^\circ$ for Fig. 5). Although the scattering is pro-

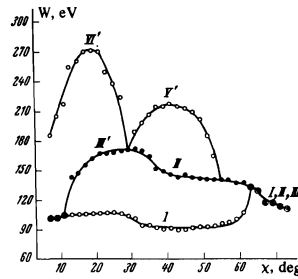


FIG. 3

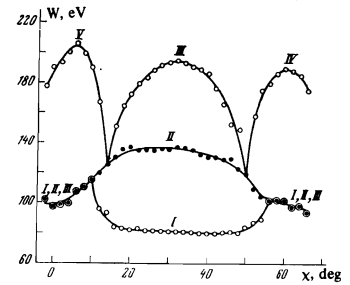
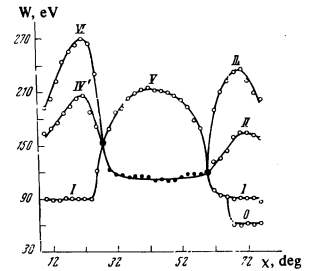


FIG. 4

FIG. 3. Energy corresponding to the positions of the maxima of peaks I, II, III, V', and VI' and the spectra of the scattered ions vs. the incidence angle of the primary ions on the surface face $\{110\}$ ($U = 580$ eV).

FIG. 4. Energy corresponding to the positions of the maxima of peaks I, II, III, IV, and V in the spectra of the scattered ions vs. the incidence angle of the primary ions on the surface face $\{001\}$ ($U = 500$ eV).

FIG. 5. Energy dependence corresponding to the positions of the maxima of peaks 0, I, II, III, IV', V, and VI in the spectra of the scattered ions vs. the incidence angle of the primary ions on the surface face $\{112\}$ ($U = 580$ eV).



duced in this case by the most closely packed directions (the interatomic distance is $\sqrt{3}a/2$, where a is the lattice constant), the maximum of curve V is close to the angle predicted by the theory of the paired interaction under the assumption that the interacting particles are infinitesimally small points, $\varphi_{000} = 44^\circ$. This last assumption should certainly be satisfied if it is assumed that the doubled paired scattering is by the less closely packed directions, namely $\langle 00\bar{1} \rangle$ (interatomic distance a) and $\langle 110 \rangle$ (distance $\sqrt{2}a$). One should therefore expect for them the value of φ_0 to lie in the interval $42 < \varphi_0 < 44^\circ$. And indeed, $\varphi_0 = 41^\circ$ for curve V' (Fig. 3), which corresponds to scattering by the neighboring atoms 4 and 5 of the chains $\langle 00\bar{1} \rangle$; if account is taken of the experimental error, this agrees with the indicated prediction.

On the other hand, no bell-shaped curve corresponding to double paired scattering by atoms 1 and 4 of the chains $\langle 110 \rangle$, with a maximum $\varphi_0 = \chi_0 \approx 41-44^\circ$, has been observed (Fig. 4). This is probably due to the larger distance between the scattered atoms in this case, when the probability of double scattering is very small^[4, 12].

The position of the maximum of φ_0 on the φ scale ($\varphi_0 = 32^\circ$) and the height ($W_0 = 195$ eV) of the bell-shaped curve for peak III (Fig. 4) agree well with the theoretical values calculated in the approximation of absolutely hard elastic spheres for group interaction with the scattering atoms 1, 4, 6, and 7 (Fig. 6), which lie in the $\{001\}$ plane ($\varphi_{0T} = 31.4^\circ$, $W_{0T} = 195$ eV, distance between the centers of the ion and of the atoms at the instant of collision is $r = 2.95 \text{ \AA}^{[11]}$). The same takes place for peak III' (Fig. 5). Analogously, the position of the maximum ($\varphi_0 = 27.5^\circ$) and the heights ($W_0 = 171$ eV) of the $W(\varphi)$ curve of peak III' (Fig. 3) are in good agreement with the theoretical values ($W_{0T} = 171$ eV, $\varphi_{0T} = 28^\circ$) calculated for a group interaction of the ion with the three atoms 4, 5, 8 of the $\{110\}$ plane (in this case $r = 2.25 \text{ \AA}$ is smaller than in the preceding case, probably because

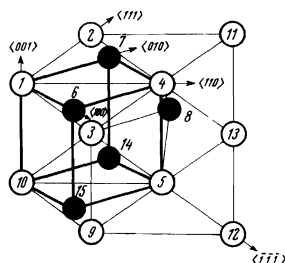


FIG. 6. Illustration of the arrangement of the atomic elements that take part in the scattering in a single crystal with BCC lattice. The ion incidence plane $\{1\bar{1}0\}$ is the plane of the figure. The atoms in this plane are represented by light circles. The atoms outside the incidence plane are represented by dark circles.

of the stronger interaction between the ion in each of the indicated atoms). The occurrence of the peaks III (Figs. 4 and 5) and III' (Fig. 3) cannot be due to double scattering that causes the ion to go outside the plane of its initial motion by colliding, for example, with atoms 1 and 6 or 4 and 8, etc., since the energy conserved by the ion in such collisions is much lower than observed in experiment ($W_0 = 90$ for the peak III and $W_0 = 70$ eV for peak III').

We note that the width of the peak III' (Fig. 2) is always much larger than the width of the other peaks, and in the region $\chi > 43^\circ$ the corresponding bell-shaped curve (Fig. 3) goes over into a relation that decreases rapidly with increasing χ . This gives grounds for assuming that there exists one more peak (III) which is not resolved by the apparatus and is due to scattering by other geometrical elements (this may be group collision with atoms 4, 8 or 8, 5). A certain confirmation of this assumption is the tendency of peak III' to split at certain values of χ .

It is probable that for the faces $\{001\}$ and $\{112\}$ the peak II is likewise due to group scattering of the ion by two lattice atoms belonging to the directions $\langle 100 \rangle$ and $\langle 010 \rangle$ (atoms 1, 6 or 1, 7).

In addition to double pair collisions, triple pair collision can also occur. If we assume, in accord with the statements made above, that the interacting particles have sufficiently small dimensions, then the "incidence angle" (between the normal to the line joining the centers of the first pair of scattering atoms and the direction of motion of the primary ion) corresponding to the maximum of the bell-shaped curve, is

$$\varphi_0 = \pi - (\psi + \beta) / 2, \quad (3)$$

where β is the angle between the segments joining respectively the centers of the first and second and of the second and third scattering atoms.

A triple interaction is possible with atoms 4, 3, and 9 for the first target and atoms 1, 10, and 9 for the second target. In both cases $\varphi_{0T} = 71.4^\circ$ and φ_{0T}

$= 71.4^\circ - 54.8^\circ = 16.6^\circ$. The experimental data (curves VI and VI') for these targets yield 18.5° and 21° respectively. The agreement is satisfactory to a sufficient degree. The reason why the difference is larger than for double collisions may be the need for involving in this case collisions with larger impact parameters when the ion is scattered by the first and third atoms. Fair agreement is obtained also for the energies W_0 , namely $W_{0T} = 252$ eV and $W_0 = 270$ eV for both targets.

The remaining peaks IV and IV' (Figs. 4 and 5) cannot be interpreted within the framework of the concepts indicated above. It is possible that they are "hybrid" peaks; peak IV (Fig. 4) can result from group scattering by atoms 1, 4, 6 and 7 at a small angle with subsequent scattering by atom 11, while peak IV' (Fig. 5) may be due to group scattering by atoms 4, 5, and 8 with subsequent scattering by atom 12.

The peak 0 (Fig. 5) is connected with double scattering with nonmonotonic variation of the direction of the scattered-ion momentum.

¹V. I. Veksler, *Fiz. Tverd. Tela* **6**, 2229 (1964) [*Sov. Phys.-Solid State* **6**, 1767 (1965)].

²V. I. Veksler, *Zh. Eksp. Teor. Fiz.* **49**, 90 (1965) [*Sov. Phys.-JETP* **22**, 65 (1966)].

³V. I. Veksler, *Izv. Akad. Nauk SSSR, seriya fiz.* **30**, 857 (1966).

⁴V. I. Veksler, *Izv. Akad. Nauk SSSR, seriya fiz.* **30**, 860 (1966).

⁵E. S. Parilis and N. Yu. Turaev, *Dokl. Akad. Nauk UzSSR No. 10*, 16 (1967); *Dokl. Akad. Nauk SSSR* **161**, 84 (1965) [*Sov. Phys.-Doklady* **10**, 212 (1965)].

⁶U. A. Arifov and A. A. Aliev, *Zh. Eksp. Teor. Fiz.* **54**, 354 (1968) [*Sov. Phys.-JETP* **27**, 190 (1968)]. *Dokl. Akad. Nauk, UzSSR No. 10*, 16 (1967); *Zh. Eksp. Teor. Fiz.* **57**, 1877 (1969) [*Sov. Phys.-JETP* **30**, 1015 (1970)].

⁷V. I. Veksler, *Vtorichnaya emissiya atomnykh chastits (Secondary Emission of Atomic Particles)*, Tashkent, Fan (1970).

⁸A. S. Avakov, S. F. Belykh, V. V. Evstifeev, and R. N. Evtukhov, *Prib. Tekh. Eksp. No. 4*, 33 (1972).

⁹*Experimental Nuclear Physics*, E. Segre, ed. **1**, Part 5, Wiley, 1953.

¹⁰N. D. Morgulis, *Zh. Tekh. Fiz.* **25**, 1667 (1955).

¹¹V. I. Veksler, *Izv. Akad. Nauk SSSR, seriya fiz.* **33**, 772 (1969).

¹²E. S. Mashkova and V. A. Molchanov, *Fiz. Tverd. Tela* **8**, 1517 (1966) [*Sov. Phys.-Solid State* **8**, 1206 (1966)].

Translated by J. G. Adashko
62